IAF-89-361

Optimal Trajectories
for the Aeroassisted Flight Experiment

A. Miele, T. Wang, W. Y. Lee, and Z. G. Zhao
Rice University, Houston, Texas
NAG8-755

40th Congress of the International
Astronautical Federation

October 7-13, 1989
Malaga, Spain

IAF-89-361

Optimal Trajectories
for the Aeroassisted Flight Experiment

A. Miele, T. Wang, W. Y. Lee, and Z. G. Zhao
Rice University, Houston, Texas

OPTIMAL TRAJECTORIES
FOR THE AEROASSISTED FLIGHT EXPERIMENT[1,2,3]

A. Miele[4], T. Wang,[5], W.Y. Lee[6], and Z. G. Zhao[7]

Rice University, Houston, Texas

Abstract. This paper deals with the determination of optimal trajectories for the aeroassisted flight experiment (AFE). The intent of this experiment is to simulate a GEO-to-LEO transfer, where GEO denotes a geosynchronous Earth orbit and LEO denotes a low Earth orbit. Specifically, the AFE spacecraft is released from the space shuttle and is accelerated by means of a solid rocket motor toward Earth, so as to achieve atmospheric entry conditions identical with those of a spacecraft returning from GEO. During the atmospheric pass, the angle of attack is kept constant, and the angle of bank is controlled in such a way that the following conditions are satisfied: (a) the atmospheric velocity depletion is such that, after exiting, the AFE spacecraft first ascends to a specified apogee and then descends to a specified perigee; and (b) the exit orbital plane is identical with the entry orbital plane. The final maneuver, not analyzed here, includes the rendezvous with and the capture by the space shuttle.

In this paper, the trajectories of an AFE spacecraft are analyzed in a 3D-space, employing the full system of 6 ODEs describing the atmospheric pass. The atmospheric entry conditions are given, and the atmospheric exit conditions are adjusted in such a way that requirements (a) and (b) are met, while simultaneously minimizing the total characteristic velocity, hence the propellant consumption required for orbital transfer. Two possible transfers are considered: (IA) indirect ascent to a 178 NM perigee via a 197 NM apogee; and

[4] Foyt Family Professor of Aerospace Sciences and Mathematical Sciences, Aero-Astronautics Group, Rice University, Houston, Texas.

[5] Senior Research Scientist, Aero-Astronautics Group, Rice University, Houston, Texas.

[6] Post-Doctoral Fellow, Aero-Astronautics Group, Rice University, Houston, Texas.

[7] Research Associate, Aero-Astronautics Group, Rice University, Houston, Texas.

(DA) direct ascent to a 178 NM apogee.

For both transfers, two cases are investigated: (i) the bank angle is continuously variable; and (ii) the trajectory is divided into segments along which the bank angle is constant. For case (ii), the following subcases are studied: two segments, three segments, four segments, and five segments; because the time duration of each segment is optimized, the above subcases involve four, six, eight, and ten parameters, respectively.

It is shown that the optimal trajectories of cases (i) and (ii) coalesce into a single trajectory: a two-subarc trajectory, with the bank angle constant in each subarc (bang-bang control). Specifically, the bank angle is near 180 deg in the atmospheric entry phase (positive lift projection phase) and is near 0 deg in the atmospheric exit phase (negative lift projection phase). It is also shown that, during the atmospheric pass, the peak values of the changes of the orbital inclination and the longitude of the ascending node are nearly zero; hence, the peak value of the wedge angle (angle between the instantaneous orbital plane and the initial orbital plane) is nearly zero. This means that the motion of the spacecraft is nearly planar in an inertial space.

Key Words. Flight mechanics, hypervelocity flight, atmospheric flight, optimal trajectories, aeroassisted flight experiment, aeroassisted orbital transfer.

1. Introduction

The field of aeroassisted orbital transfer (AOT) has received considerable attention in recent years. See for example Refs. 5-9 and references therein. In this paper, which is based on Refs. 1-4, the problem of the optimal trajectories of an AFE vehicle is formulated, solved, and analyzed.

The aeroassisted flight experiment (AFE) refers to the study of the free flight of an autonomous spacecraft, shuttle-launched and shuttle-recovered. Its purpose is to gather atmospheric entry data for use in designing aeroassisted orbital transfer vehicles (AOTV). The intent of this experiment is to simulate a GEO-to-LEO transfer, where GEO denotes a geosynchronous Earth orbit and LEO denotes a low Earth orbit (Refs. 10-11).

In an actual AOT transfer, GEO-to-LEO, the maneuver is initiated with a propulsive impulse at GEO so as to decelerate the spacecraft and force it into an elliptical transfer orbit leading to atmospheric entry. In a simulated AOT transfer, GEO-to-LEO, the maneuver is initiated by releasing the spacecraft from the space shuttle, which is flying at the altitude of 160 NM above the Earth surface. By means of a solid rocket motor, the AFE spacecraft is accelerated toward Earth, so as to achieve atmospheric entry conditions identical with those of a spacecraft returning from GEO. Thus, for the purposes of this paper, the atmospheric entry

conditions are to be considered as given.

During the atmospheric pass, the angle of attack of the AFE spacecraft is kept at the constant value $\alpha = 17$ deg. This value is such that the lift L is negative. Control of the AFE spacecraft is achieved via the angle of bank μ. Hence, the projected lift $L_p = L\cos\mu$ (the vertical component of the lift vector) can be made positive or negative at will, depending on the value of μ.

The time history of the control, the bank angle $\mu(t)$, is subject to two requirements: (a) the atmospheric velocity depletion must be such that, after exiting, the AFE spacecraft first ascends to a specified apogee and then descends to a specified perigee; and (b) the exit orbital plane must be identical with the entry orbital plane; this is the same as stating that the exit value of the wedge angle must vanish; see Ref.10. Here, one additional requirement is considered: (c) the propellant consumption required for orbital transfer must be as small as possible, implying that the characteristic velocity ΔV must be as small as possible; in turn, minimizing ΔV is equivalent to maximizing the exit value of the horizontal component of the inertial velocity; this implies either maximizing the exit value of the inertial velocity or minimizing the exit value of the inertial path inclination.

In this paper, the optimal trajectories of the AFE spacecraft are determined with reference to a 3D-space and employing the full system of 6 ODEs describing the atmospheric pass. In the general formulation of Refs. 1-2, the effects due to the rotation of the Earth and the oblateness of the Earth are included. In this paper, the former are included, but the latter are excluded, since they have been found to be small. The resulting optimal control problem is solved by means of the sequential gradient-restoration algorithm (SGRA, Refs. 12-14). While this algorithm is available in both the primal formulation and the dual formulation, the former is used in this paper, based on previous experience with various AOT problems (see for example Refs. 15-17).

Using SGRA, the optimal trajectories are computed for two possible transfers: (IA) indirect ascent to a 178 NM perigee via a 197 NM apogee; and (DA) direct ascent to a 178 NM apogee. For each transfer, two cases are investigated: (i) the bank angle is continuously variable; hence, $\mu(t)$ is treated as a control; and (ii) the trajectory is divided into segments along which the bank angle is constant; hence, for each segment, μ is treated as a parameter. For case (ii), the following subcases are studied: 2, 3, 4, 5 segments; because the time duration of each segment is also a parameter to be optimized, the above subcases involve 4, 6, 8, 10 parameters, respectively.

For comparison purposes and only for Transfer (IA), a reference trajectory is also considered: this is a 5-segment trajectory, close to the nominal trajectory

given in Ref. 10.

To sum up, this paper considers ten optimal trajectories, five for Transfer (IA) and five for Transfer (DA). These optimal trajectories are compared with (and are found to be superior to) the reference trajectory in terms of the main quantities of interest, namely: total characteristic velocity, peak heating rate, peak dynamic pressure, peak change of orbital inclination, peak change of the longitude of the ascending node, and peak value of the wedge angle.

Content. Section 2 contains the notations. The system description is given in Section 3, and the optimization problem is formulated in Section 4. The experimental data are given in Section 5, and the numerical results are presented in Section 6. Finally, the conclusions are given in Section 7.

2.   Notations

Throughout this paper, the following notations are employed:

C_D = drag coefficient;

C_L = lift coefficient;

D = drag, N;

g = local acceleration of gravity, m/sec^2;

h = altitude, m;

i = orbital inclination, rad;

L = lift, N;

m = mass, kg;

r = radial distance from the center of the Earth, m;

r_e = radius of the Earth, m;

r_a = radius of the outer edge of the atmosphere, m;

S = reference surface area, m^2;

t = time, sec;

V = velocity, m/sec;

V_a = circular velocity at $r = r_a$, m/sec;

α = angle of attack, rad;

γ = path inclination, rad;

η = wedge angle, rad;

θ = longitude, rad;

μ = bank angle, rad;

μ_e = Earth's gravitational constant, m^3/sec^2;

ρ = air density, kg/m^3;

τ = final time, sec;

ϕ = latitude, rad;

χ = heading angle, rad;

ω = angular velocity of the Earth, rad/sec;

Ω = longitude of the ascending node, rad;

ΔV = characteristic velocity, m/sec.

Subscripts

0 = entry into the atmosphere;

1 = exit from the atmosphere;

11 = perigee for Transfer (IA) or apogee for Transfer (DA);

22 = apogee for Transfer (IA).

Superscripts

· = derivative with respect to time;

~ = quantity defined in an inertial system.

Acronyms

AFE = aeroassisted flight experiment;

AFEV = aeroassisted flight experiment vehicle;

AOT = aeroassisted orbital transfer;

AOTV = aeroassisted orbital transfer vehicle;

DA   = direct ascent;

DP   = dynamic pressure, N/m^2;

GEO = geosynchronous Earth orbit;

HEO = high Earth orbit;

HR = heating rate, W/m^2;

IA = indirect ascent;

LAN = longitude of the ascending node, rad;

LEO = low Earth orbit;

ODE = ordinary differential equation;

OT = optimal trajectory;

RT = reference trajectory;

SGRA = sequential gradient-restoration algorithm;

WA = wedge angle, rad.

3. System Description

The motion of the AFE spacecraft takes place partly in the atmosphere and partly in space. For the purposes of this paper, the initial point is the atmospheric entry point; it corresponds to GEO return conditions and is fixed; the final point is located at the altitude of 178 NM and corresponds to circularization into LEO. We consider two transfer maneuvers: (IA) indirect ascent to a 178 NM perigee via a 197 NM apogee; and (DA) direct ascent to a 178 NM apogee.

For Transfer (IA), the key points of the maneuver are these:point 0, atmospheric entry; point 1, atmospheric exit; point 22, apogee (h = 197 NM) of the first post-atmospheric transfer orbit; and point 11, perigee (h = 178 NM) of the second post-atmospheric transfer orbit. Propulsive impulses are applied at two points: at the apogee 22 in order to raise the height of the perigee; and at the perigee 11 in order to circularize the motion.

For Transfer (DA), the key points of

the maneuver are these: point 0, atmospheric entry; point 1, atmospheric exit; and point 11, apogee (h = 178 NM) of the post-atmospheric transfer orbit. A propulsive impulse is applied at only one point: at the apogee 11 in order to circularize the motion.

For the atmospheric portion (h $\leq$ h_a) of the trajectory of the AFE spacecraft,we employ an Earth-fixed system; for the space portion of the trajectory (h $\geq$ h_a), we employ an inertial system; here, h_a = 400,000 ft $\cong$ 121.9 km denotes the thickness of the atmosphere. For h $\leq$ h_a, we compute the air density using the US Standard Atmosphere, 1976 (Ref. 18); for h $\geq$ h_a,we assume that the air density is zero. For both the atmospheric portion and the space portion of the trajectory, we neglect the effects due to the oblateness of the Earth; we assume that the gravitational field is central and obeys the inverse square law.

Atmospheric Pass. With reference to the atmospheric portion of the trajectory of the AFE vehicle, the following additional hypotheses are employed: (a) the atmospheric pass is made with engine shut-off; hence, the AFE spacecraft behaves as a particle of constant mass; (b) the angle of attack is constant, α = 17 deg; (c) under extreme hypersonic conditions, the dependence of the aerodynamic coefficients on the Mach number and the Reynolds number is disregarded; (d) the sideslip angle is zero; hence, the side force component of the aerodynamic force is zero. The only control is the angle of bank μ.

<u>Differential System</u>. With the above assumptions and upon using an Earth-fixed system, the equations of motion include the kinematical equations

$$\dot{\theta} = V\cos\gamma \, \cos\chi/r\cos\phi, \tag{1a}$$

$$\dot{\phi} = -V\cos\gamma \, \sin\chi/r, \tag{1b}$$

$$\dot{r} = V\sin\gamma, \tag{1c}$$

and the dynamical equations

$$\dot{V} = -D/m - g\sin\gamma$$
$$+\omega^2 r(\sin\gamma\cos^2\phi+\cos\gamma\sin\chi\cos\phi\sin\phi), \tag{1d}$$

$$\dot{\gamma} = (L/mV)\cos\mu+(V/r-g/V)\cos\gamma+2\omega\cos\chi\cos\phi$$
$$+(\omega^2 r/V)(\cos\gamma\cos^2\phi-\sin\gamma\sin\chi\cos\phi\sin\phi), \tag{1e}$$

$$\dot{\chi} = (L/mV)\sin\mu/\cos\gamma+(V/r)\cos\gamma\cos\chi\tan\phi$$
$$+2\omega(\sin\phi+\tan\gamma\sin\chi\cos\phi)$$
$$+(\omega^2 r/V)\cos\chi\cos\phi\sin\phi/\cos\gamma. \tag{1f}$$

In the dynamical equations, the symbol ω denotes the angular velocity of the Earth; terms linear in ω are due to the Coriolis acceleration; terms quadratic in ω are due to the transport acceleration. Also in the dynamical equations, the acceleration of gravity is given by

$$g = \mu_e/r^2, \tag{2}$$

where μ_e denotes the Earth's gravitational constant. In addition, the aerodynamic forces are given by

$$D = (1/2)C_D(\alpha)\rho(h)SV^2, \tag{3a}$$

$$L = (1/2)C_L(\alpha)\rho(h)SV^2, \tag{3b}$$

where the air density ρ depends on the altitude h, with

$$h = r - r_e. \tag{3c}$$

Since α is constant, both the drag coefficient and the lift coefficient are constant. The control of the spacecraft is the angle of bank μ. Equations (1) must be integrated, subject to (2) and (3), over the time interval $0 \le t \le \tau$. Here, the initial time $t = 0$ corresponds to atmospheric entry; and the final time $t = \tau$ corresponds to atmospheric exit.

<u>Transformation Relations</u>. The following transformation relations allow one to pass from quantities computed in an Earth-fixed system to quantities computed in an inertial system, and viceversa:

$$\tilde{\theta} = \theta + \omega t, \tag{4a}$$

$$\tilde{\phi} = \phi, \tag{4b}$$

$$\tilde{r} = r, \tag{4c}$$

$$\tilde{V}\cos\tilde{\gamma}\cos\tilde{\chi} = V\cos\gamma\cos\chi + \omega r\cos\phi, \tag{4d}$$

$$\tilde{V}\cos\tilde{\gamma}\sin\tilde{\chi} = V\cos\gamma\sin\chi, \tag{4e}$$

$$\tilde{V}\sin\tilde{\gamma} = V\sin\gamma. \tag{4f}$$

The first three equations are linear and refer to the state variables appearing in the kinematical equations. The next three equations are nonlinear and refer to the state variables appearing in the dynamical equations; in spite of the nonlinearity, these equations can be solved explicitly

to yield $\tilde{V}$, $\tilde{\gamma}$, $\tilde{\chi}$ in terms of V, γ, χ, and viceversa. This step is omitted for the sake of brevity; see Refs. 1-2.

Orbital Elements. Once the state variables are known in the inertial system, one can compute some important orbital quantities such as the orbital inclination i and the longitude of the ascending node Ω. These quantities are supplied by the relations

$$\cos i = \cos\phi \cos\tilde{\chi}, \tag{5a}$$

$$\sin(\tilde{\theta} - \Omega) = \cot i \tan\phi. \tag{5b}$$

Another important quantity is the wedge angle η, which is the angle between the instantaneous orbital plane and the entry orbital plane. This angle is given by

$$\cos\eta = \sin i \sin i_0 \cos(\Omega-\Omega_0) + \cos i \cos i_0. \tag{5c}$$

Summary. To sum up, in the Earth-fixed system, the equations governing the atmospheric pass include the differential system (1) and the analytical and functional relations (2)-(3). In this formulation, the independent variable is the time t, $0 \le t \le \tau$. The dependent variables include six state variables $[\theta(t)$, $\phi(t)$, $r(t)$, $V(t)$, $\gamma(t)$, $\chi(t)]$, one control variable $[\mu(t)]$, and one parameter (τ). If the initial values of the state variables are given and if the bank angle program is prescribed, the system can be integrated in forward time. Then, using (4), one can convert the state variables computed in the Earth-fixed system into state variables computed in the inertial system. Finally,

using (5), one can determine the orbital inclination, the longitude of the ascending node, and the wedge angle.

Initial Conditions. At atmospheric entry, the initial values of the state variables $\tilde{\theta}_0$, ϕ_0, $r_0 = r_a$, $\tilde{V}_0$, $\tilde{\gamma}_0$, $\tilde{\chi}_0$ are given in the inertial system. Hence, the initial values of the orbital elements i_0, Ω_0 are known. By definition, the initial value of the wedge angle satisfies the relation $\eta_0 = 0$. Using the transformation relations (4), the initial values of the state variables θ_0, ϕ_0, $r_0 = r_a$, V_0, γ_0, χ_0 become known in the Earth-fixed system.

Final Conditions. The final time τ is free and is to be determined indirectly as the time instant at which the spacecraft exits from the atmosphere; hence,

$$r_1 = r_a. \tag{6a}$$

Application of energy conservation and angular momentum conservation to the exit-to-apogee transfer orbit yields either the relation

$$\text{(IA)} \quad r_{22}^2(2\tilde{v}_a^2-\tilde{v}_1^2)-2r_{22}r_a\tilde{v}_a^2+r_a^2\tilde{v}_1^2\cos^2\tilde{\gamma}_1 = 0 \tag{6b}$$

or the relation

$$\text{(DA)} \quad r_{11}^2(2\tilde{v}_a^2-\tilde{v}_1^2)-2r_{11}r_a\tilde{v}_a^2+r_a^2\tilde{v}_1^2\cos^2\tilde{\gamma}_1 = 0. \tag{6c}$$

Equation (6b) applies to the indirect ascent case; Equation (6c) applies to the direct ascent case. These relations guarantee that, after exiting, the spacecraft ascends to the specified apogee.

Finally, the orbital plane at atmospheric exit must be identical with the orbital plane at atmospheric entry; hence, the exit value of the wedge angle must vanish,

$$\eta_1 = 0. \tag{6d}$$

Use of the transformation relations (4) in conjunction with (5) allows one to transform the final conditions (6) to include quantities computed in the Earth-fixed system.

4. Optimal Control Problem

Subject to the previous constraints, different optimal control problems can be formulated, depending on the performance index chosen and the type of transfer maneuver considered. Here, we focus attention on the minimization of the total characteristic velocity ΔV, which is a measure of the propellant consumption required for orbital transfer.

Problem (IA). This problem refers to the indirect ascent to a 178 NM perigee via a 197 NM apogee. The functional to be minimized is given by

$$I = \Delta V = \Delta V_{22} + \Delta V_{11}, \tag{7a}$$

with

$$\Delta V_{22} = \tilde{V}_a \sqrt{[2 r_a r_{11} / (r_{11} r_{22} + r_{22}^2)]}$$

$$- (r_a / r_{22}) \tilde{V}_1 \cos \tilde{\gamma}_1, \tag{7b}$$

$$\Delta V_{11} = \tilde{V}_a \sqrt{[2 r_a r_{22} / (r_{11} r_{22} + r_{11}^2)]}$$

$$- \tilde{V}_a \sqrt{(r_a / r_{11})}. \tag{7c}$$

Problem (DA). This problem refers to the direct ascent to a 178 NM apogee. The functional to be minimized is given by

$$I = \Delta V = \Delta V_{11}, \tag{8a}$$

with

$$\Delta V_{11} = \tilde{V}_a \sqrt{(r_a / r_{11})} - (r_a / r_{11}) \tilde{V}_1 \cos \tilde{\gamma}_1. \tag{8b}$$

Alternative Formulations. Inspection of the performance indexes (7) and (8) shows that they include a constant part and a part which is linear in the exit value of the horizontal component of the inertial velocity $\tilde{V}_h = \tilde{V} \cos \tilde{\gamma}$. Hence, the minimization of ΔV is equivalent to maximizing the functional

$$J = \tilde{V}_{h1} = \tilde{V}_1 \cos \tilde{\gamma}_1. \tag{9a}$$

In turn, because of the final conditions (6b) or (6c), the maximization of the functional (9a) implies either maximizing the functional

$$K = \tilde{V}_1 \tag{9b}$$

or minimizing the functional

$$H = \tilde{\gamma}_1. \tag{9c}$$

Continuous vs Discrete Control. For both Problems (IA) and (DA), two cases are investigated: continuous control and discrete control.

(i) Continuous Control. Here, the bank angle is continuously variable. Hence, $\mu(t)$ is treated as a control variable.

(ii) Discrete Control. Here, the trajectory is divided into s segments along which the bank angle is constant; hence, for each segment, the bank angle μ_i is treated as a parameter. Because the

time duration τ_i of each segment is also a parameter to be optimized, the number of parameters is twice the number of segments. The following subcases are studied: s = 2, 3, 4, 5. These subcases involve n_p = 4, 6, 8, 10 parameters, respectively.

Algorithm. For both cases (i) and (ii), Problems (IA) and (DA) are optimal control problems of the Bolza type. They can be solved using the sequential gradient-restoration algorithm (SGRA, Refs. 12-14) employed in conjunction with the primal formulation (PSGRA, Ref. 14).

The sequential gradient-restoration algorithm is an iterative technique which involves a sequence of cycles, each cycle including two phases: the gradient phase and the restoration phase. In the gradient phase, the value of the augmented functional is decreased, while avoiding excessive constraint violation. In the restoration phase, the value of the constraint error is decreased, while avoiding excessive change in the value of the functional. In a complete gradient-restoration cycle, the value of the functional is decreased, while the constraints are satisfied to a preselected degree of accuracy. Thus, a succession of suboptimal solutions is generated, each new solution being an improvement over the previous one from the point of view of the value of the functional being minimized.

The convergence conditions are represented by the relations

$$P \leq \varepsilon_1, \qquad Q \leq \varepsilon_2. \tag{10}$$

Here, P is the norm squared of the error in the constraints; Q is the norm squared of the error in the optimality conditions; and ε_1, ε_2 are preselected small, positive numbers.

5. Experimental Data

The following data were used in the numerical experiment (for more significant digits, see Ref. 4).

Earth's Physical Constants. The radius of the Earth is r_e = 6378 km; the radius of the outer edge of the atmosphere is r_a = 6500 km; the thickness of the atmosphere is h_a = 121.9 km; the Earth's gravitational constant is μ_e = 0.3986E+15 m^3/sec^2; the circular velocity at $r = r_a$ is $\tilde{V}_a$ = 7.831 km/sec; the angular velocity of the Earth is ω = 0.7292E-04 rad/sec.

Spacecraft Data. The mass of the AFE spacecraft is m = 1678 kg; the reference surface area is S = 14.31 m^2; the spacecraft flies at constant angle of attack, α = 17.00 deg; the lift coefficient is C_L =-0.3707; and the drag coefficient is C_D = 1.315.

Atmospheric Model. The assumed atmospheric model is that of the US Standard Atmosphere, 1976 (Ref. 18). In this model, the values of the density are tabulated at discrete altitudes. For intermediate altitudes, the density is computed by assuming an exponential fit for the function $\rho(h)$.

Heating Rate. The stagnation point heating rate is assumed to be given by the formula

$$HR = C\sqrt{(\rho/\rho_R)} (V/V_R)^{3.07}. \tag{11}$$

Here, ρ_R is a reference density, the density at $h_R = 60$ km; $V_R = \tilde{V}_a$ is a reference velocity; the constant C represents the stagnation point heating rate at $\rho = \rho_R$ and $V = V_R$ and is given by $C = 282.3$ W/cm^2; note that the value of this constant is based on a nose radius of one foot.

Atmospheric Entry Conditions. In the inertial system, the given initial conditions are as follows: the longitude is $\tilde{\theta}_0 = -134.52$ deg; the latitude is $\phi_0 = -4.49$ deg; the altitude is $h_0 = 121.9$ km; the radius is $r_0 = 6500$ km; the velocity is $\tilde{V}_0 = 10.31$ km/sec; the path inclination is $\tilde{\gamma}_0 = -4.49$ deg; the heading angle is $\tilde{\chi}_0 = -28.13$ deg; the orbital inclination is $i_0 = 28.45$ deg; the longitude of the ascending node is $\Omega_0 = -126.19$ deg; the wedge angle is $\eta_0 = 0.00$ deg.

Atmospheric Exit Conditions. In the inertial system, the desired final conditions are as follows: the altitude is $h_1 = 121.9$ km; the radius is $r_1 = 6500$ km; the orbital inclination is $i_1 = 28.45$ deg; the longitude of the ascending node is $\Omega_1 = -126.19$ deg; the wedge angle is $\eta_1 = 0.00$ deg.

Transfer (IA). This is the indirect ascent to a 178 NM perigee via a 197 NM apogee. The required apogee conditions are as follows: the altitude is $h_{22} = 364.8$ km; the radius is $r_{22} = 6743$ km; and the path inclination is $\tilde{\gamma}_{22} = 0.00$ deg. The required perigee conditions are as follows: the altitude is $h_{11} = 329.7$ km; the radius is

$r_{11} = 6708$ km; and the path inclination is $\tilde{\gamma}_{11} = 0.00$ deg.

Transfer (DA). This is the direct ascent to a 178 NM apogee. The required apogee conditions are as follows: the altitude is $h_{11} = 329.7$ km; the radius is $r_{11} = 6708$ km; and the path inclination is $\tilde{\gamma}_{11} = 0.00$ deg.

6. Numerical Results

The optimal control problem formulated in Sections 3-4 was solved with the sequential gradient-restoration algorithm for the experimental data outlined in Section 5. Both Transfer (IA) and Transfer (DA) were optimized from the point of view of the characteristic velocity ΔV. For each transfer, five optimal trajectories (OT) were computed: the continuous control OT; the discrete control OT with $s = 2$ segments; the discrete control OT with $s = 3$ segments; the discrete control OT with $s = 4$ segments; and the discrete control OT with $s = 5$ segments. For Transfer (IA), a reference trajectory (RT) was also computed; this is a nonoptimal discrete-control trajectory with $s = 5$ segments, obtained by means of the restoration algorithm, starting from a nominal traject-ory supplied in Ref.10. Thus, a total of 11 trajectories were computed, ten optimal trajectories and one reference trajectory. The numerical results are shown in Tables 1-2 and Figs. 1-2.

Table 1 shows the values of the characteristic velocity ΔV and the flight time τ for all the trajectories computed.

For Transfer (IA), the reference trajectory requires $\Delta V = 98.0$ m/sec and a flight time $\tau = 488$ sec; also for Transfer (IA), the optimal trajectories require $\Delta V = 81.9$ m/sec and a flight time $\tau = 796$ sec. For Transfer (DA), the optimal trajectories require $\Delta V = 72.0$ m/sec and a flight time $\tau = 820$ sec. To sum up, the optimal trajectories are considerably more efficient propulsively than the reference trajectory and they are characterized by a longer flight time.

An interesting result of the analysis is that, for each transfer, the optimal continuous-control trajectory and the optimal discrete-control trajectories coalesce into a single trajectory: a two-subarc trajectory, with the bank angle constant in each subarc (bang-bang control). Specifically, the bank angle is near 180 deg in the atmospheric entry phase (positive lift projection phase) and is near 0 deg in the atmospheric exit phase (negative lift projection phase). This is true for both Transfer (IA) and Transfer (DA). See Figs. 1-2.

In the light of the above statement, we now focus attention on only three trajectories: for Transfer (IA), the re-ference trajectory and the two-subarc optimal trajectory; for Transfer (DA), the two-subarc optimal trajectory. For these trajectories, Table 2 shows the values of the following quantities: the character-istic velocity; the flight time; the minimum altitude; the peak dynamic pressure; the peak heating rate; the peak change of the orbital inclination; the peak change of the longitude of the ascending node; and the peak value of the wedge angle.

Table 2 illustrates clearly the advantages of the OTs with respect to the reference trajectory. Concerning the longitudinal motion, by comparison with the RT, the OTs are characterized by smaller ΔV and also by smaller values of the peak dynamic pressure and the peak heating rate; this is due to the fact that the minimum altitude of the OTs is about 3 km higher than the minimum altitude of the RT. Concerning the lateral motion, by comparison with the RT, the OTs exhibit smaller values of the peak change of the orbital inclination and the peak change of the longitude of the ascending node; hence, the peak wedge angle of the OTs is smaller than the corresponding quantity for the RT. Indeed, it is suprising that $\max|\Delta i|$ and $\max|\Delta\Omega|$ are nearly zero for the OTs; hence, $\max(\eta)$ is nearly zero for the OTs. This means that, for efficient flight, the motion of the spacecraft must be nearly planar in an inertial space; in other words, one must avoid energy dissipation associated with the lateral motion.

More details on the trajectories computed can be found in Figs. 1 and 2. Figure 1 refers to Transfer (IA), and Fig. 2 refers to Transfer (DA). These figures include the time histories of the following quantities: the bank angle (Figs. 1A and 2A); the altitude (Figs. 1B and 2B); the

relative velocity (Figs. 1C and 2C); the relative path inclination (Figs. 1D and 2D); the dynamic pressure (Figs. 1E and 2E); the heating rate (Figs. 1F and 2F); and the wedge angle (Figs. 1G and 2G).

Remark. With reference to the two-subarc OTs of Transfer (IA) and Transfer (DA), we observe that the value of the bank angle is $\mu = 176.7$ deg for the atmospheric entry phase and $\mu = 5.5$ deg for the atmospheric exit phase. Let L denote the lift, and let

$$L_p = L\cos\mu, \qquad L_q = L\sin\mu \qquad (12)$$

denote the vertical component and the lateral component of the lift. Let C_L, C_{Lp}, C_{Lq} denote the associated lift coefficients, and observe that

$$C_{Lp} = C_L\cos\mu, \qquad C_{Lq} = C_L\sin\mu. \qquad (13)$$

We recall that the AFE spacecraft flies at constant angle of attack $\alpha = 17$ deg, corresponding to $C_L = -0.3707$ and $C_D = 1.315$. With this understanding, we see that, for the atmospheric entry phase,

$$C_{Lp} = -0.998\ C_L, \qquad C_{Lq} = 0.058\ C_L; \qquad (14)$$

and we see that, for the atmospheric exit phase,

$$C_{Lp} = 0.995\ C_L, \qquad C_{Lq} = 0.096\ C_L. \qquad (15)$$

Therefore, the following comments arise:

(i) in the atmospheric entry phase, the vertical component of the lift is directed upward and its modulus is only 2/1000 smaller than the lift modulus; this causes the path inclination to increase

gradually from the entry negative value to nearly zero value;

(ii) in the atmospheric exit phase, the vertical component of the lift is directed downward and its modulus is only 5/1000 smaller than the lift modulus; this offsets the centrifugal force effects due to the curvature of the Earth, so as to ensure exit conditions compatible with the desired apogee requirement;

(iii) the lateral component of the lift during the atmospheric entry phase and the lateral component of the lift during the atmospheric exit phase have the same sign and the same order of magnitude; their modulus is 5.8% of the lift modulus in the atmospheric entry phase and 9.6% of the lift modulus in the atmospheric exit phase; these lateral lift components are directed in such a way that they nearly offset the effects due to the Earth's rotation, so as to ensure exit conditions compatible with the desired wedge angle requirement.

7. Conclusions

In this paper, the trajectories of an AFE spacecraft are analyzed in a 3D-space, employing the full system of 6 ODEs describing the atmospheric pass. It is assumed that the angle of attack is constant and that the spacecraft is controlled via only the angle of bank. It is also assumed that the atmospheric entry conditions are given and that the atmospheric exit conditions are adjusted in such a way that the following conditions are satisfied: (a) the atmospheric velocity depletion is such

that, after exiting, the AFE spacecraft first ascends to a specified apogee and then descends to a specified perigee; and (b) the exit orbital plane is identical with the entry orbital plane.

Under the above conditions, optimal trajectories are determined by minimizing the total characteristic velocity, hence the propellant consumption required for orbital transfer. The resulting optimization problems are solved by means of the sequential gradient-restoration algorithm.

Two possible transfers are considered: (IA) indirect ascent to a 178 NM perigee via a 197 NM apogee; and (DA) direct ascent to a 178 NM apogee. For both transfers, two cases are investigated: (i) the bank angle is continuously variable; and (ii) the trajectory is divided into segments along which the bank angle is constant. For cases (ii), the following subcases are studied: two segments, three segments, four segments, and five segments; because the time duration of each segment is optimized, the above subcases involve four, six, eight, and ten parameters, respectively. For comparison purposes and only for Transfer (IA), a reference trajectory is also considered: this is a five-segment trajectory, close to the nominal trajectory given in Ref. 10.

From the extensive numerical computations, the following conclusions arise:

(i) The optimal trajectories are two-subarc trajectories, with the bank angle constant in each subarc; hence, the control is bang-bang.

(ii) In the atmospheric entry phase, the bank angle is near 180 deg, yielding a positive projected lift, which in turn causes the path inclination to increase gradually from the entry negative value to nearly zero value.

(iii) In the atmospheric exit phase, the bank angle is near 0 deg, yielding a negative projected lift, which offsets the centrifugal force effects due to the curvature of the Earth, so as to ensure exit conditions compatible with the desired apogee requirement.

(iv) The lateral component of the lift during the atmospheric entry phase and the lateral component of the lift during the atmospheric exit phase have the same sign and the same order of magnitude; they are directed in such a way that they nearly offset the effects due to the Earth's rotation. In this way, the instantaneous orbital plane is almost identical with the initial orbital plane, meaning that the wedge angle is nearly zero during the atmospheric pass. This means that, for efficient flight, the motion of the AFE spacecraft is nearly planar in an inertial space; in other words, one must avoid energy dissipation associated with the lateral motion.

(v) Comparison of the optimal trajectories and the reference trajectory shows that the OTs are superior to the RT in terms of the main quantities of interest, namely, the characteristic velocity, the peak dynamic pressure, the peak heating

rate, and the peak wedge angle. In part-
icular, for Transfer (IA), the charact-
eristic velocity is $\Delta V = 98.0$ m/sec for
the RT and $\Delta V = 81.9$ m/sec for the OT. For
Transfer (DA), the characteristic velocity
of the OT is 72.0 m/sec.

References

1.   MIELE, A., ZHAO, Z. G., and LEE,
     W. Y., "Optimal Trajectories for the
     Aeroassisted Flight Experiment, Part
     1, Equations of Motion in an Earth-
     Fixed System", Rice University, Aero-
     Astronautics Report No. 238, 1989.

2.   MIELE, A., ZHAO, Z. G., and LEE,
     W. Y., "Optimal Trajectories for the
     Aeroassisted Flight Experiment, Part
     2, Equations of Motion in an Inertial
     System", Rice University, Aero-
     Astronautics Report No. 239, 1989.

3.   MIELE, A., WANG, T., LEE, W. Y., and
     ZHAO, Z. G., "Optimal Trajectories
     for the Aeroassisted Flight Experi-
     ment, Part 3, Formulation, Results,
     and Analysis", Rice University, Aero-
     Astronautics Report No. 242, 1989.

4.   MIELE, A., WANG, T., LEE, W. Y., WANG,
     H., and WU, G. D., "Optimal Traject-
     ories for the Aeroassisted Flight
     Experiment, Part 4, Data, Tables,
     and Graphs", Rice University, Aero-
     Astronautics Report No. 243, 1989.

5.   WALBERG, G. D., "A Survey of Aero-
     assisted Orbital Transfer", Journal
     of Spacecraft and Rockets, Vol. 22,
     No. 1, pp. 3-18, 1985.

6.   MEASE, K. D., and VINH, N. X.,
     "Minimum-Fuel Aeroassisted Coplanar
     Orbital Transfer Using Lift Modulat-
     ion", Journal of Guidance, Control,
     and Dynamics, Vol. 8, No. 1, pp. 134-
     141, 1985.

7.   VINH, N. X., and HANSON, J. M.,
     "Optimal Aeroassisted Return from High
     Earth Orbit with Plane Change", Acta
     Astronautica, Vol. 12, No. 1, pp. 11-
     25, 1985.

8.   MIELE, A., Editor, "Special Issue on
     Hypervelocity Flight", Journal of the
     Astronautical Sciences, Vol. 36, Nos.
     1-2, pp. 1-197, 1988.

9.   MEASE, K. D., "Optimization of Aero-
     assisted Orbital Transfer: Current
     Status", Journal of the Astronautical
     Sciences, Vol. 36, Nos. 1-2, pp. 7-34,
     1988.

10. ANONYMOUS, N. N., "Aeroassisted Flight
     Experiment: Preliminary Design Docu-
     ment", NASA Marshall Space Flight
     Center, 1986.

11. GAMBLE, J. D., CERIMELE, C. J., MOORE,
     T. E., and HIGGINS, J., "Atmospheric
     Guidance Concepts for an Aeroassist
     Flight Experiment", Journal of the
     Astronautical Sciences, Vol. 36, Nos.
     1-2, pp. 45-71, 1988.

12. MIELE, A., and WANG, T., "Primal-Dual
     Properties of Sequential Gradient-
     Restoration Algorithms for Optimal
     Control Problems, Part 1, Basic
     Problem", Integral Methods in Science
     and Engineering, Edited by

F. R. Payne et al, Hemisphere
Publishing Corporation, Washington,
DC, pp. 577-607, 1986.

13. MIELE, A., and WANG, T., "Primal-Dual
Properties of Sequential Gradient-
Restoration Algorithms for Optimal
Control Problems, Part 2, General
Problem", Journal of Mathematical
Analysis and Applications, Vol. 119,
Nos. 1-2, pp. 21-54, 1986.

14. MIELE, A., WANG, T., and BASAPUR,
V. K., "Primal and Dual Formulations
of Sequential Gradient-Restoration
Algorithms for Trajectory Optimizat-
ion Problems", Acta Astronautica,
Vol. 13, No. 8, pp. 491-505, 1986.

15. MIELE, A., BASAPUR, V. K., and MEASE,
K. D., "Nearly-Grazing Optimal
Trajectories for Aeroassisted Orbital
Transfer", Journal of the Astro-
nautical Sciences, Vol. 34, No. 1,
pp. 3-18, 1986.

16. MIELE, A., BASAPUR, V. K., and LEE,
W. Y., "Optimal Trajectories for
Aeroassisted, Coplanar Orbital
Transfer", Journal of Optimization
Theory and Applications, Vol. 52,
No. 1, pp. 1-24, 1987.

17. MIELE, A., BASAPUR, V. K., and LEE,
W. Y., "Optimal Trajectories for
Aeroassisted, Noncoplanar Orbital
Transfer", Acta Astronautica, Vol. 15,
Nos. 6-7, pp. 399-411, 1987.

18. NOAA, NASA, and USAF, "US Standard
Atmosphere, 1976", US Government
Printing Office, Washington, DC, 1976.

Supplementary References

19. LONDON, H. S., "Change of Satellite
Orbit Plane by Aerodynamic Maneuvering",
Journal of the Aerospace Sciences,
Vol. 29, No. 3, pp. 323-332, 1962.

20. HULL, D. G., GILTNER, J. M., SPEYER,
J. L., and MAPAR, J., "Minimum-Energy-
Loss Guidance for Aeroassisted Orbital
Plane Change", Journal of Guidance,
Control, and Dynamics, Vol. 8, No. 4,
pp. 487-493, 1985.

21. CALISE, A. J., "Singular Perturbation
Analysis of the Atmospheric Orbital Plane
Change Problem", Journal of the
Astronautical Sciences, Vol. 36, Nos.
1-2, pp. 35-43, 1988.

22. HULL, D. G., McCLENDON, J. R., and
SPEYER, J. L., "Aeroassisted Orbital
Plane Change Using an Elliptic Drag
Polar", Journal of the Astronautical
Sciences, Vol. 36, Nos. 1-2, pp. 73-
87, 1988.

23. MEASE, K. D., LEE, J. Y., and VINH,
N. X., "Orbital Changes during Hyper-
velocity Aerocruise", Journal of the
Astronautical Sciences, Vol. 36, Nos.
1-2, pp. 103-137, 1988.

24. VINH, N. X., and LU, P., "Chebyshev
Minimax Problems for Skip Traject-
ories", Journal of the Astronautical
Sciences, Vol. 36, Nos. 1-2, pp. 179-
197, 1988.

Table 1. Characteristic velocity and flight time.

Trajectory	Control	s	ΔV (m/sec)	τ (sec)
IART	Discrete	5	97.97	487.6
IAOT	Continuous	∞	81.86	795.3
IAOT	Discrete	2	81.86	795.7
IAOT	Discrete	3	81.86	795.7
IAOT	Discrete	4	81.86	795.8
IAOT	Discrete	5	81.84	796.2
DAOT	Continuous	∞	72.05	817.6
DAOT	Discrete	2	72.03	819.5
DAOT	Discrete	3	72.03	819.6
DAOT	Discrete	4	72.03	819.6
DAOT	Discrete	5	72.01	819.9

IA = indirect ascent,   DA = direct ascent,
OT = optimal trajectory,   RT = reference trajectory,
s = number of segments.

Table 2. Comparison of AFE trajectories.

Quantity	IART s = 5	IAOT s = 2	DAOT s = 2	Units
ΔV	97.97	81.86	72.03	m/sec
τ	487.6	795.7	819.5	sec
min(h)	74.6	77.5	77.5	km
max(DP)	1629	1174	1174	N/m^2
max(HR)	158	148	148	W/cm^2
max$|\Delta i|$	1.08	0.01	0.01	deg
max$|\Delta\Omega|$	0.32	0.00	0.00	deg
max(η)	1.08	0.01	0.01	deg

IA = indirect ascent,   DA = direct ascent,
OT = optimal trajectory,   RT = reference trajectory,
s = number of segments.
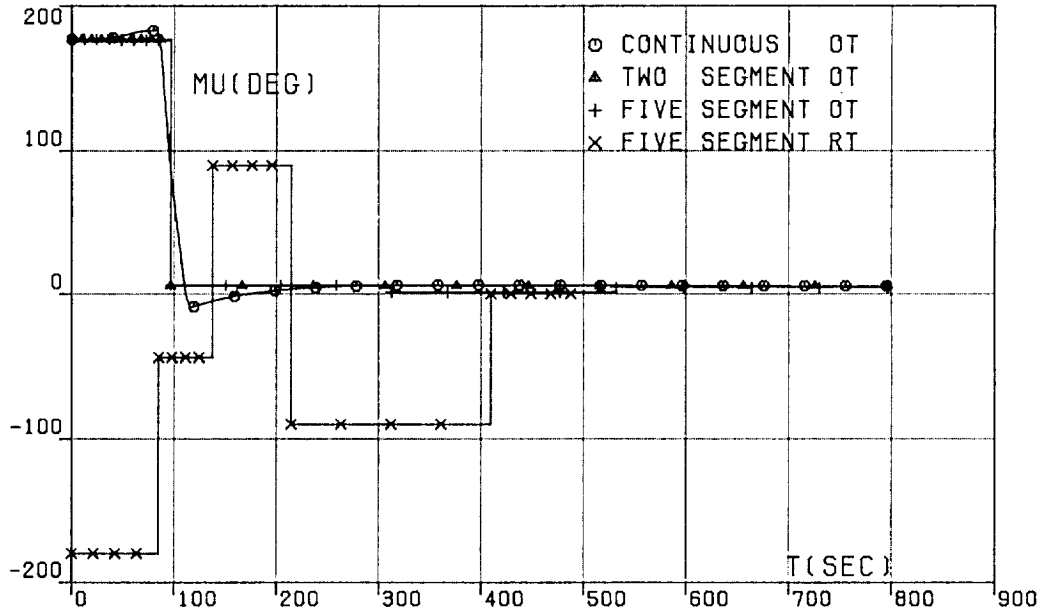
FIG.1A. COMPARISON OF AFE TRAJECTORIES,
TRANSFER (IA), BANK ANGLE.
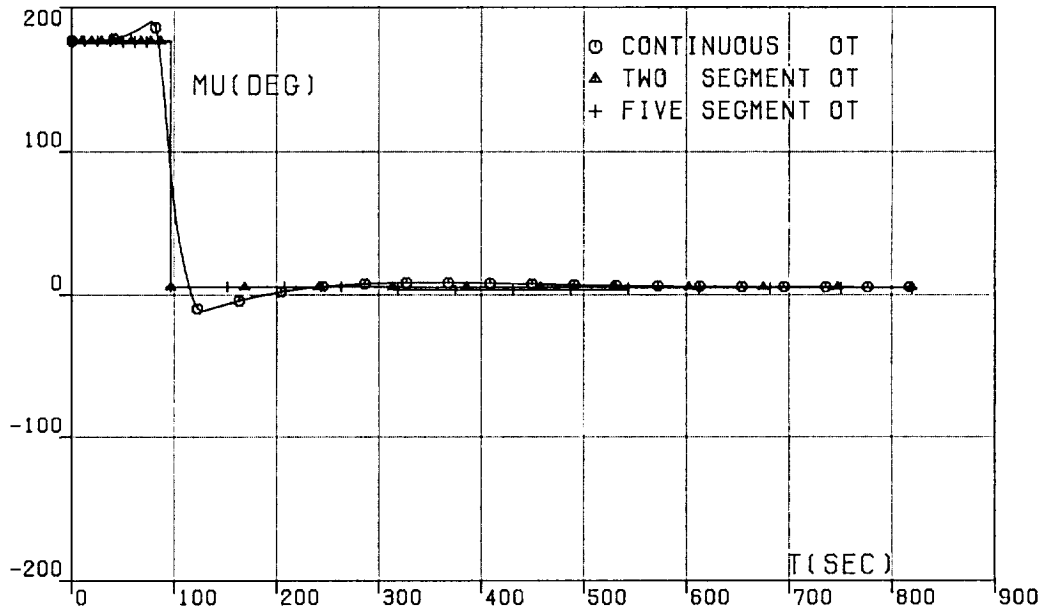
FIG.2A. COMPARISON OF AFE TRAJECTORIES,
TRANSFER (DA), BANK ANGLE.
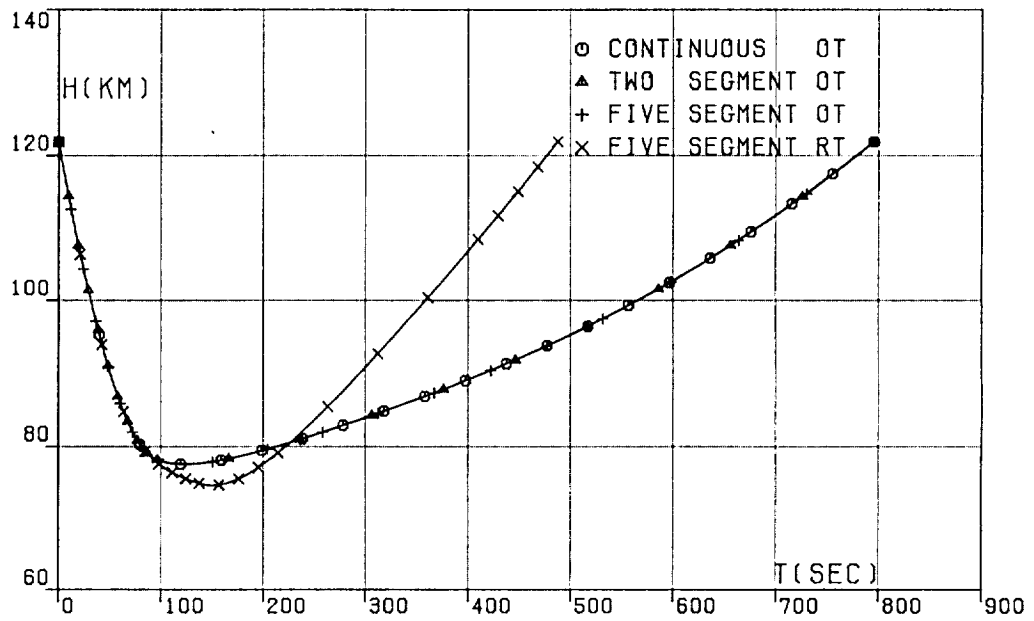
FIG.1B. COMPARISON OF AFE TRAJECTORIES,
TRANSFER (IA), ALTITUDE.
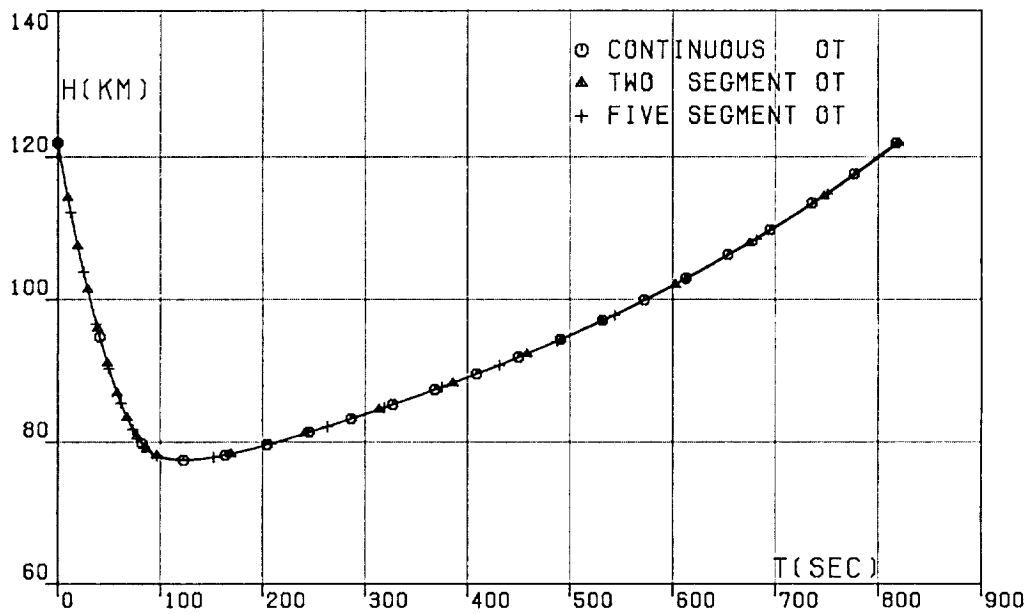
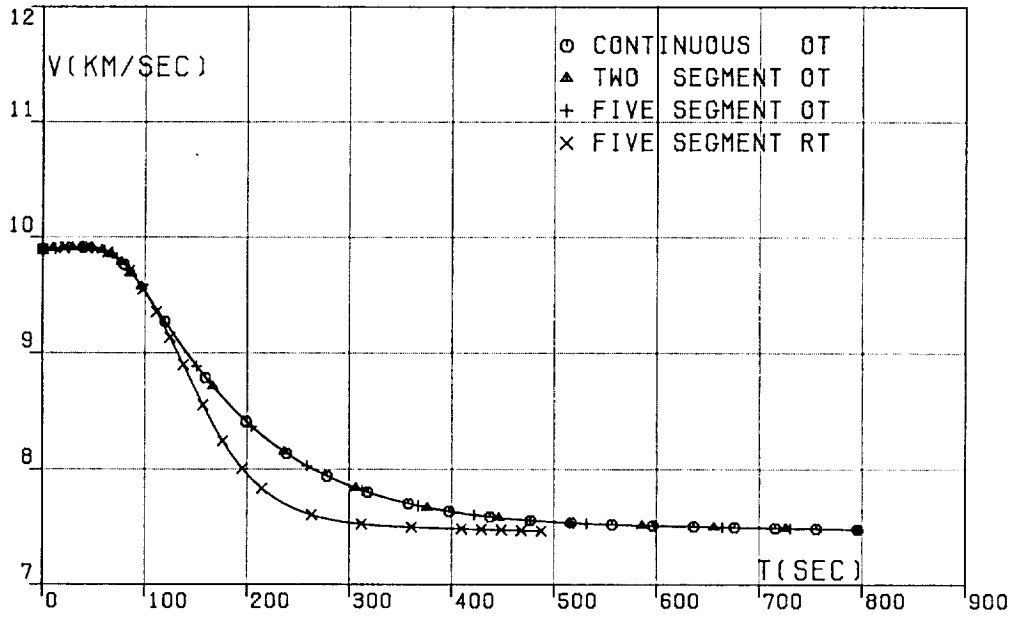FIG.2B. COMPARISON OF AFE TRAJECTORIES,
TRANSFER (DA), ALTITUDE.

FIG.1C. COMPARISON OF AFE TRAJECTORIES,
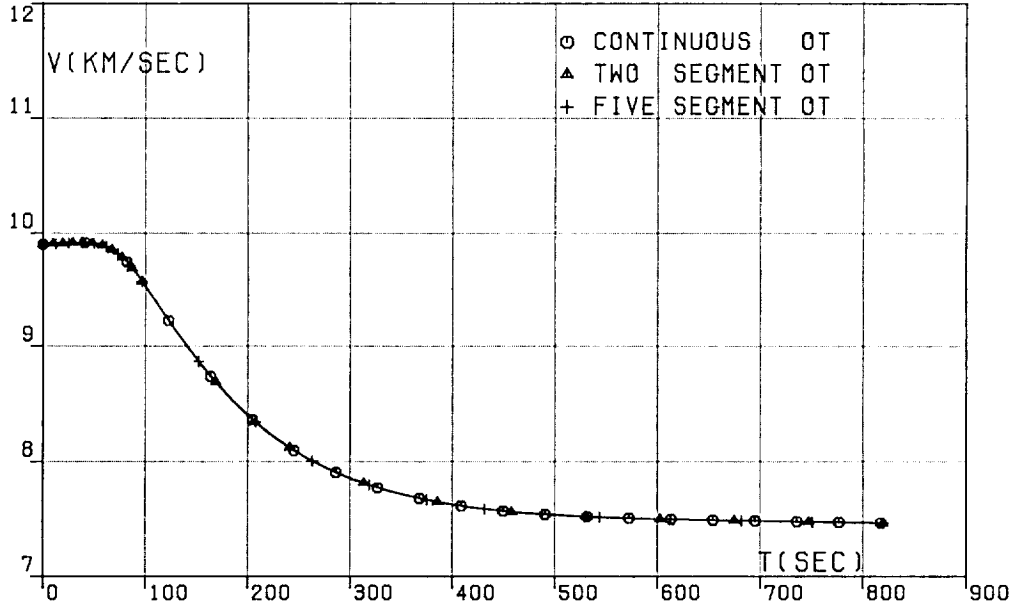TRANSFER (IA), VELOCITY, RELATIVE.

FIG.2C. COMPARISON OF AFE TRAJECTORIES,
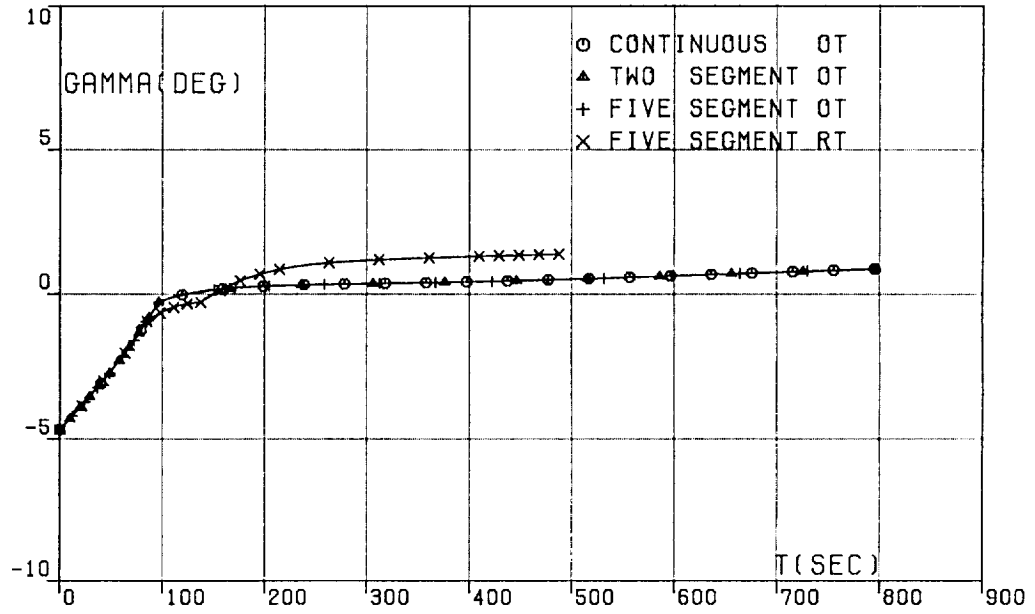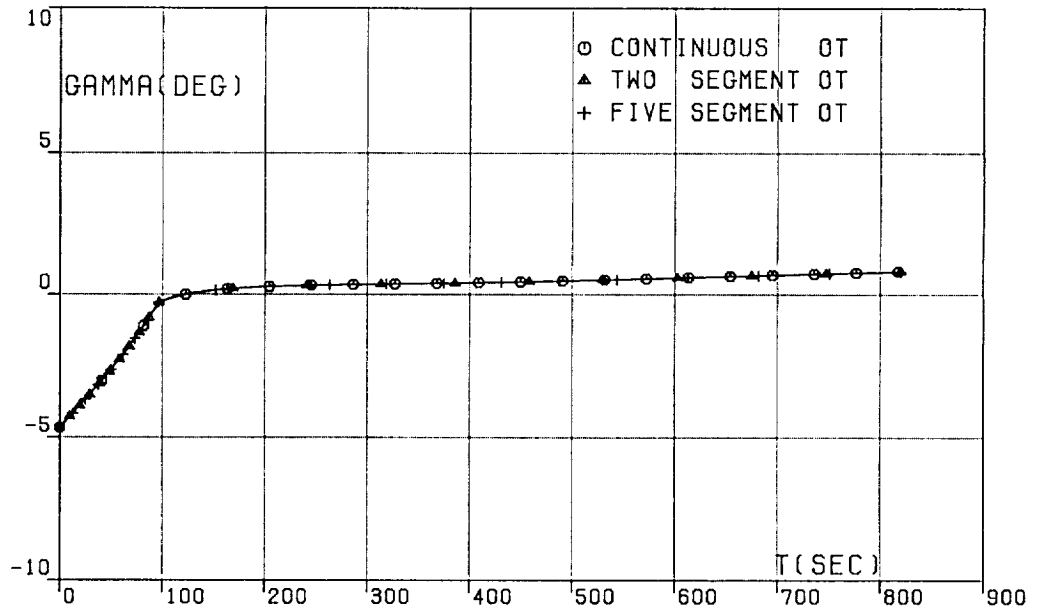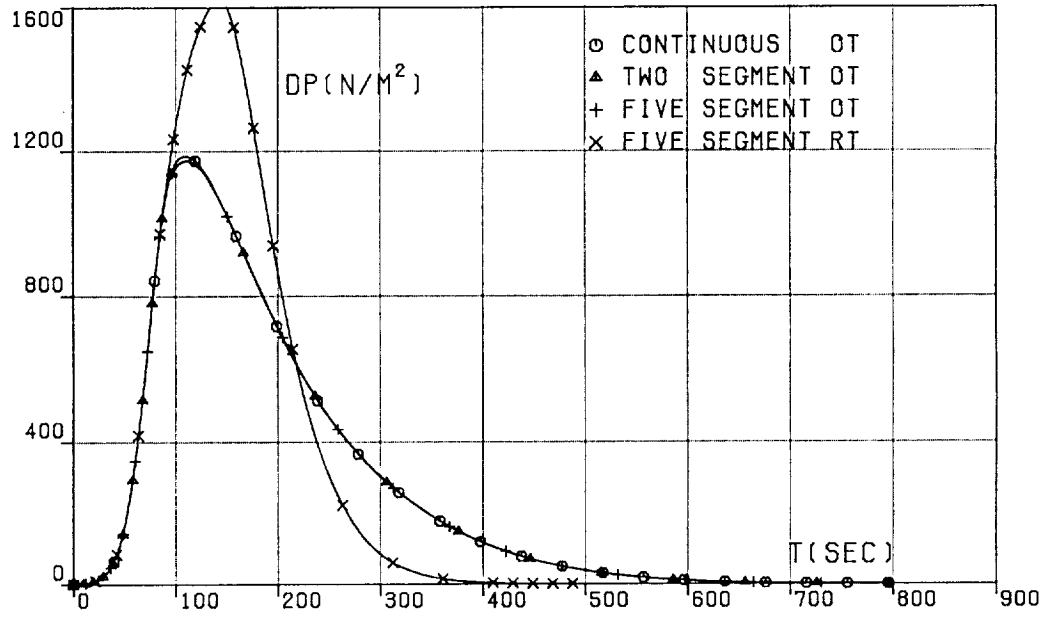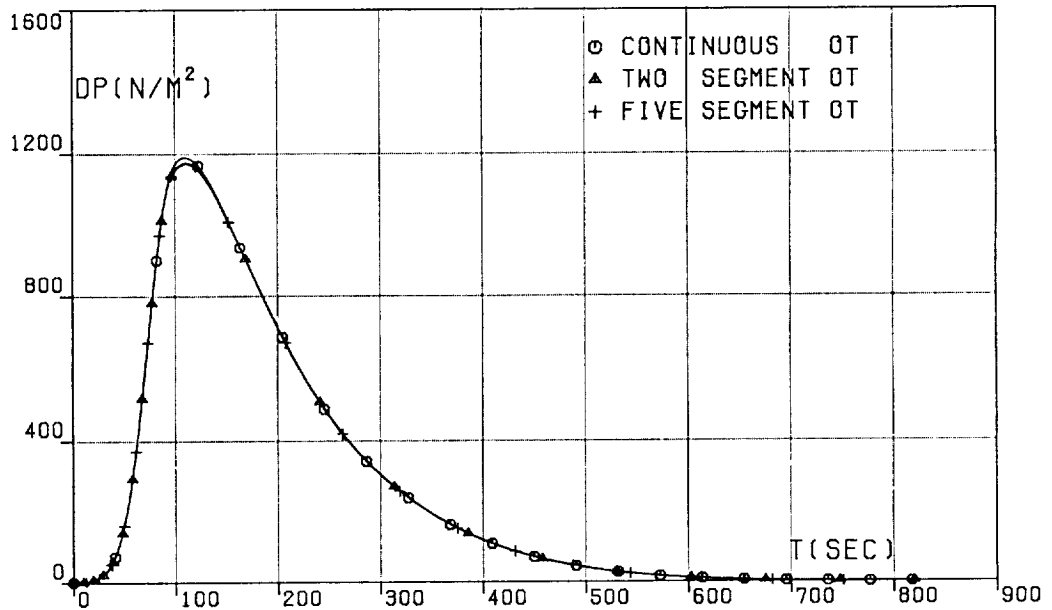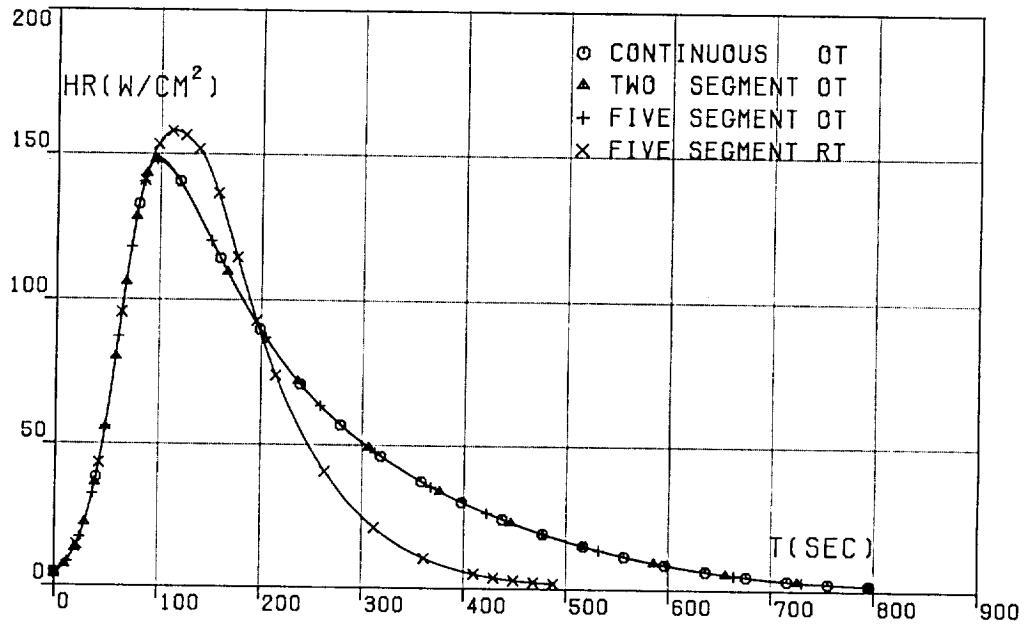TRANSFER (DA), VELOCITY, RELATIVE.

FIG.1D. COMPARISON OF AFE TRAJECTORIES,
          TRANSFER (IA),
          PATH INCLINATION, RELATIVE.

FIG.2D. COMPARISON OF AFE TRAJECTORIES,
          TRANSFER (DA),
          PATH INCLINATION, RELATIVE.

FIG.1E. COMPARISON OF AFE TRAJECTORIES.
TRANSFER (IA), DYNAMIC PRESSURE.

FIG.2E. COMPARISON OF AFE TRAJECTORIES,
TRANSFER (DA), DYNAMIC PRESSURE.

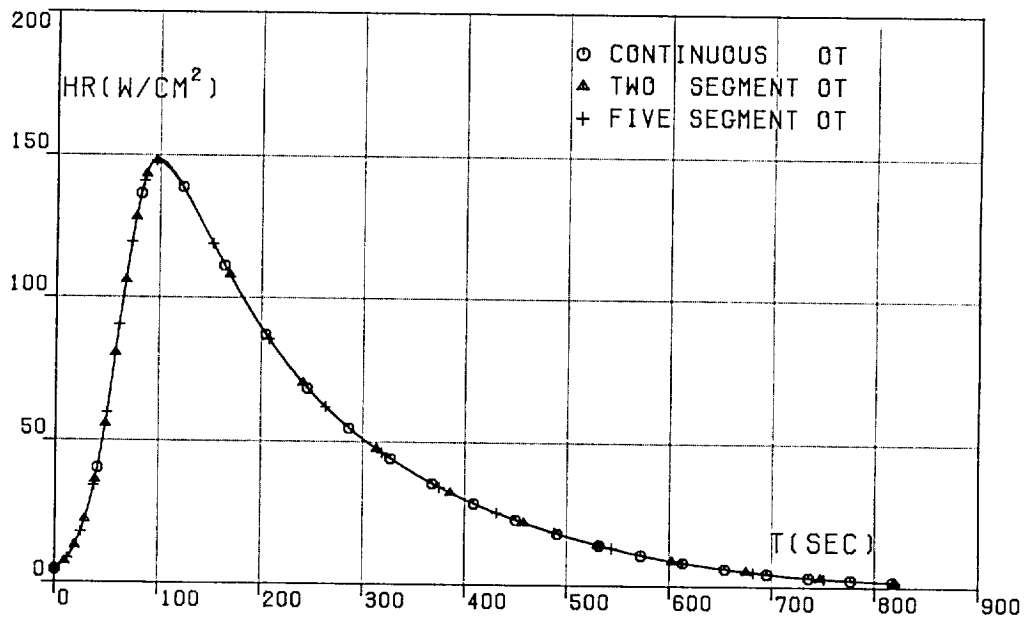FIG.1F. COMPARISON OF AFE TRAJECTORIES,
TRANSFER (IA), HEATING RATE.

FIG.2F. COMPARISON OF AFE TRAJECTORIES,
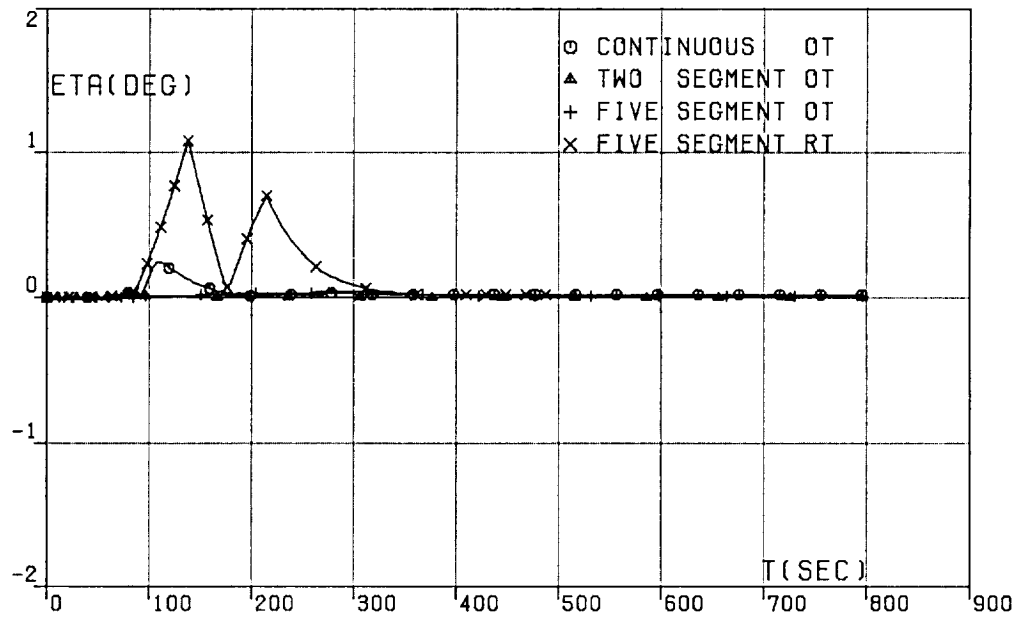TRANSFER (DA), HEATING RATE.
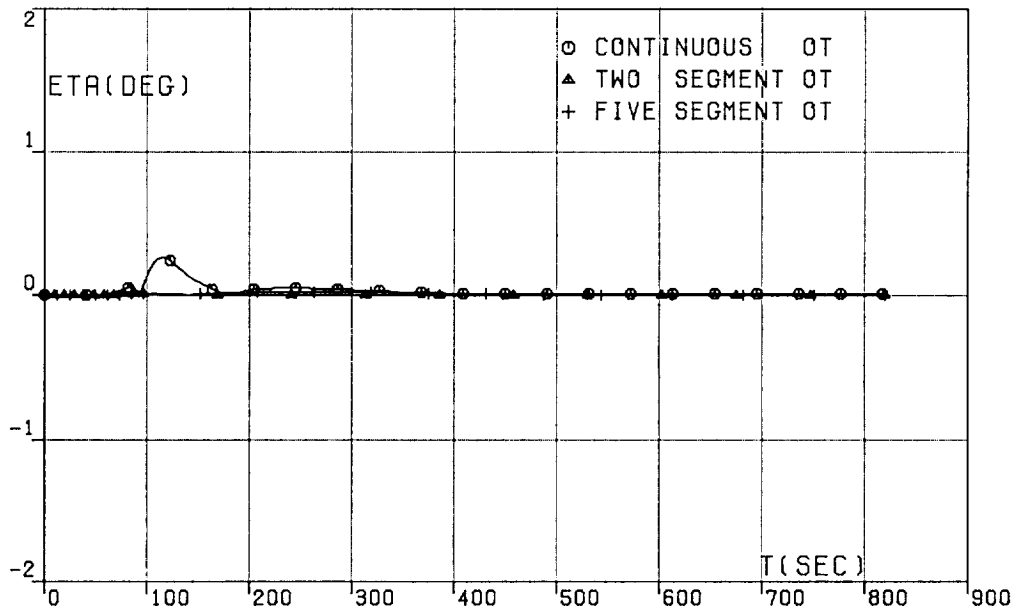
FIG.1G. COMPARISON OF AFE TRAJECTORIES,
TRANSFER (IA), WEDGE ANGLE.

FIG.2G. COMPARISON OF AFE TRAJECTORIES,
TRANSFER (DA), WEDGE ANGLE.